JOURNAL OF AGRICULTURAL AND FOOD CHEMISTRY

J. Agric. Food Chem. **2008,** *56,* 9949–9961 **9949**

Metabolic Changes in Roots of the Oilseed Canola Infected with the Biotroph *Plasmodiophora brassicae*: Phytoalexins and Phytoanticipins

M. Soledade C. Pedras,*,† Qing-An Zheng,† and Stephen Strelkov‡

Department of Chemistry, University of Saskatchewan, 110 Science Place, Saskatoon, SK, S7N 5C9, Canada, and Department of Agricultural, Food and Nutritional Science, University of Alberta, Edmonton, Alberta T6G 2P5, Canada

Analyses of metabolite production and accumulation in roots of canola (*Brassica napus* L. spp. *oleifera*) infected with the phytopathogen *Plasmodiophora brassicae* (clubroot) allowed the identification of 45 metabolites. HPLC analysis corroborated by metabolite isolation and NMR spectroscopic data demonstrated for the first time that phytoalexins and phytoanticipins were produced in roots of canola infected with a soilborne biotroph. In addition, six new indolyl metabolites were identified, synthesized, and tested against three fungal pathogens of canola. Multivariate data analysis using principal component analysis (PCA) revealed distinct metabolic responses of canola to *P. brassicae* infection during a six-week period. At late harvest days (five and six weeks), a clear clustering was observed among samples of infected roots because of the higher concentration of phytoalexins, while higher concentration of phytoanticipins contributed to the differentiation between three and four weeks samples of infected and control roots. Altogether, the data shows that canola roots under biotrophic attack are able to produce a complex blend of phytoalexins and other antimicrobial metabolites as a defensive response and that the metabolic regulation of phytoanticipins and phytoalexins appeared to correlate with the infection period.

KEYWORDS: Canola; cyclobrassinin; phytoalexin; phytoanticipin; *Plasmodiophora brassicae*

INTRODUCTION

Oilseed crucifers, particularly *Brassica* species, are of great importance worldwide because of the variety and quality of edible and industrial oils as well as protein content of crushed seed, which is widely used for animal feed. Canola (*Brassica napus* L. and *B. rapa* L.) acreage has increased substantially across the world during the last decades and is likely to continue playing an important role in agriculture trade. Crucifers, including canola, produce complex blends of secondary metabolites involved in defense pathways against pathogens and pests. Phytoalexins are antimicrobial defense metabolites produced *de novo* in response to biotic and abiotic stresses (*1*), whereas phytoanticipins are constitutive defenses whose production may increase under stress (*2*). All currently known crucifer phytoalexins contain an indole or oxoindole nucleus, whereas phytoanticipins display a much broader range of structures, including aliphatic and aromatic isothiocyanates (*2*).

Plasmodiophora brassicae is a soilborne biotroph that causes clubroot, one of the most damaging root diseases of crucifer crops. *P. brassicae* occurs worldwide and has an extensive host range, including canola (*3*) and wild crucifers such as *Arabidopsis thaliana.* Resting spores of *P. brassicae* can survive in the soil for many years until susceptible roots that support their germination emerge (*3*). Germinated spores release motile zoospores that form plasmodia inside the root cells leading to abnormal cell division and characteristic galls. The root clubs inhibit nutrient and water transport, which stunts plant growth and leads to eventual death (*4*). The development of clubroot disease symptoms appears to correlate with an increase in the plant hormones indolyl-3-acetic acid and cytokinin and depend on several factors. The total indolyl-3-acetic acid content is higher in infected roots than in noninfected roots, particularly at earlier infection stages. Although the biosynthetic origin of both plant hormones remains elusive, it appears that the cytokinin required for the formation of large clubroots is produced by *P. brassicae* (*4, 5*). In addition, cloning of isoforms of nitrilases from *B. rapa* and their differential expression during clubroot development indicated their role in clubroot disease (*6*). Proteome-level changes in the roots of canola as a result of *P. brassicae* infection showed changes in the amounts of several proteins relative to controls (*7*). These proteins were involved in lignin biosynthesis, cytokinin metabolism, glycolysis, intracellular calcium homeostasis, and detoxification of reactive oxygen species. For example, about a 6-fold reduction in caffeoyl-CoA *O*-methyltransferase production suggested a re-

* Corresponding author. Tel: (306)966-4772. Fax: (306)966-4730. E-mail: s.pedras@usask.ca.

† University of Saskatchewan.

‡ University of Alberta.

10.1021/jf802192f CCC: $40.75
Published on Web 10/04/2008

duction in host lignin biosynthesis after pathogen challenge (*7*). Furthermore, a recent study using *A. thaliana* ecotypes and a double mutant deficient in both indole glucosinolates (GSLs) and camalexin production showed that the infection rate and disease index as a measure of club development was similar in both wild type and mutant plants (*8*). Hence, it was suggested that camalexin and indole GSLs were not crucial factors influencing gall development in infected roots of *A. thaliana*. Camalexin is the main phytoalexin produced in some wild crucifers, including *A. thaliana*, whereas indolyl GSLs are phytoanticipins characteristic of the family Brassicaceae (*2*). Nonetheless, since several crucifer metabolites do not appear to be produced in *A. thaliana*, questions regarding the significance of the phytoalexin and phytoanticipin biosynthetic pathways in clubroot can only be answered if cultivated *Brassica* species are analyzed.

Obligate biotrophs such as *P. brassicae* can penetrate and colonize plant host tissues in ways that prevent immediate recognition by the host. For example, a biotroph may induce production or suppression of different proteins in the host and suppress induced resistance mechanisms such as phytoalexin production and hypersensitive host cell death (*9*). Recently, analysis of metabolites produced in leaves of canola and rapeseed (*B. rapa* L.) inoculated with different races of the biotroph *Albugo candida* demonstrated that complex blends of phytoalexins (spirobrassinin, cyclobrassinin, and rutalexin) and phytoanticipins (indolyl-3-acetonitrile, arvelexin, caulilexin C, and 4-methoxyglucobrassicin) were produced consistently (*10*). However, because analysis of plant defense pathways involving phytoalexin and phytoanticipin accumulation during biotrophic infections has been carried out in very few systems, generalizations cannot be made yet. This knowledge could provide metabolic leads useful to improve plant tolerance or resistance to biotrophic pathogens or novel metabolic targets to control biotrophs. Toward this end, we have investigated the kinetics of metabolite production and accumulation (polar and nonpolar) in roots of canola during infection with *P. brassicae* and identified 45 metabolites, six of which are new indolyl metabolites. These new metabolites were synthesized and tested against three fungal pathogens of canola. In addition, we demonstrate for the first time that canola roots under biotrophic attack are able to produce a complex blend of phytoalexins and other antimicrobial metabolites as a defensive response. Distinct defense pathways involving up and down regulation of the biosynthesis of indolyl phytoanticipins and phytoalexins were revealed through PCA analysis.

MATERIALS AND METHODS

General Procedures. All chemicals were purchased from Sigma-Aldrich Canada Ltd., Oakville, ON. All solvents were HPLC grade and used as such. Solvents used in syntheses were dried over the following drying agents prior to use: benzene, THF, and Et_2O over sodium/benzophenone. Organic extracts were dried over Na_2SO_4 and solvents removed under reduced pressure in a rotary evaporator.

NMR spectra were recorded on 500 MHz spectrometers. For ^1H NMR spectra (500 MHz), the chemical shifts (δ) are reported in parts per million (ppm) relative to TMS. The δ values were referenced to $CDCl_3$ ($CHCl_3$ at 7.28 ppm), CD_3CN (CD_2HCN at 1.94 ppm), and CD_3OD (CD_2HOD at 3.31 ppm). For ^{13}C NMR (125.8 MHz), the chemical shifts (δ) were referenced to $CDCl_3$ (77.4 ppm) and CD_3OD (49.0 ppm). The multiplicities of the ^{13}C signals refer to the number of attached protons: $s = C$; $d = CH$; $t = CH_2$; and $q = CH_3$. Fourier transform infrared (FT-IR) data were recorded on a spectrometer, and spectra were measured by the diffuse reflectance method on samples dispersed in KBr. Ultraviolet (UV) spectra were recorded on a spectrophotometer using a 1 cm path length quartz cell. Optical rotation $[\alpha]_D$ was determined at ambient temperature on a Perkin-Elmer 141 polarimeter using a 1 mL, 10 dm cell.

Materials. Seeds of canola (*Brassica napus* cv. Westar) were obtained from Agricultural and Agri-Food Canada, Saskatoon Research Centre, SK, Canada. A field isolate (SACAN03−1) representing pathotype 3 of *Plasmodiophora brassicae* (*11*), as defined on the differentials of Williams, was obtained from University of Alberta, Canada. Seeds were placed on wet filter paper in Petri dishes (100 di × 20 mm, each dish containing ca. 50 seeds). The Petri dishes were kept under constant light at 23 °C. After 7 days, the seedlings were either inoculated with a resting-spore suspension of *P. brassica*e or used as controls. To prepare spore suspensions, frozen clubroots (10 g) were soaked in water (50 mL, autoclaved). After 30 min, roots were cut into small pieces and ground using a blender. After filtration through eight layers of cheesecloth, the aqueous suspension containing resting spores (ca. 10^7 spores/mL) was kept at 4 °C overnight (*11*).

The seedlings were inoculated with spores by dipping roots in spore suspensions (aqueous) for 60 s, were transferred to pots containing a soil mixture (Sunshine LG-3, Washington, USA; containing 70−80% Canadian sphagnum peat moss, vermiculite, dolomitic limestone, gypsum, and wetting agent), and grown in a growth chamber. Control seedlings (noninoculated) were dipped in autoclaved water, planted, and grown similarly. Growth cabinet conditions: day/night temperature 22/16 °C, ambient humidity, 16 h photoperiod with light intensity at 250 μmol s^{-1} m^{-2}. Roots of infected and control plants were harvested 2 weeks after planting and every week up to 6 weeks.

Extraction of Plant Material. Three inoculated plants were combined to make one analytical sample and triplicate samples were prepared for analysis of three to six weeks after inoculation and after planting roots. Although typical clubroot symptoms are not observed on canola until three weeks after initial infection, 2-week post-inoculation roots were also analyzed (a larger number of plants was required per sample due to the size of roots; thus, only duplicate samples were available). Control plants were collected and processed in a manner similar to that for inoculated plants. Roots were washed carefully with distilled water to remove soil, dried between filter paper, cut, and weighed. After cutting into small pieces, roots were frozen in liquid nitrogen, freeze-dried, and ground into a fine powder using a glass rod. Roots were extracted with methanol (10 mL × 2) with sonication, each time for 20 min. After filtration, the combined methanol extracts were concentrated under reduced pressure, and the residue was extracted with CH_2Cl_2 (2 × 3 mL). The remaining residue (not soluble in CH_2Cl_2) was dissolved in MeOH-H_2O (1:1, 1.0 mL) and was filtered to yield the polar fraction for HPLC analysis. The CH_2Cl_2 fraction was concentrated under reduced pressure, and the residue was dissolved in acetonitrile (200 μL) to yield the nonpolar fraction for HPLC analysis. Samples were analyzed using reverse-phase (RP) HPLC coupled to diode array detector (DAD) and electrospray ionization (ESI) ion-trap mass spectrometry detector (HPLC-ESI-MS), as described below. Leaves of control and infected canola were also extracted for phytoalexin and phytoanticipin analysis.

HPLC-DAD Analysis. HPLC analysis was performed using an HP 1050 HPLC system (Agilent Technology, US) equipped with a DAD. Separation (23 °C) was carried out on a Eclipse XSB C-18 column (5 μm particle size silica, 150 mm × 4.6 mm) equipped with an online filter. Eluant A consisted of 0.1% TFA in H_2O, and eluant B consisted of 0.1% TFA in acetonitrile at a flow rate of 1.0 mL/min. The injection volume was set to 10 μL. For analysis of nonpolar (NP) metabolites, the method NP was used: linear gradient elution starting with 75:25 of A/B to 25:75 of A/B in 35 min, to 100% B in 5 min, and a flow rate 1.0 mL/min. For analysis of polar (PP) metabolites the method PP was used: linear gradient elution starting with 100% of A, reaching 70:30 A/B in 25 min, and a flow rate of 1.0 mL/min.

HPLC-ESI-MS Analysis. An Agilent 1100 HPLC system coupled to an LC/MSD ion trap detector with electrospray ionization was used. Chromatographic separation was carried out at room temperature using an Eclipse XSB C-18 column (5 μm particle size silica, 150 mm × 4.6 mm) equipped with an online filter. The mobile phase consisted of a gradient of 0.2% formic acid in H_2O (A) and 0.2% formic acid in acetonitrile (B). The injection volume was set to 10 μL. Method NP-

MS was developed for the analysis of nonpolar metabolites: linear gradient elution starting with 75:25 of A/B to 25:75 of A/B in 35 min, to 100% B in 5 min, and a flow rate 1.0 mL/min. Method PP-MS was developed for polar metabolites: linear gradient elution starting with 100% of A, reaching 70:30 A/B in 25 min, and a flow rate of 1.0 mL/min. The ion mode was set as positive and negative. The interface and MSD detector parameters were as follows: nebulizer pressure, 70.0 psi (N_2); dry gas, N_2 (12.0 L/min); dry gas temperature, 350 °C; spray capillary voltage 3500 V; skimmer voltage, 40.0 V; ion transfer capillary exit, 100 V; scan range, *m/z* 100−1000. Ultrahigh pure He was used as the collision gas. Data were acquired in positive and negative modes in a single LC run, using the continuous polarity switching ability of the mass spectrometer. Samples dissolved in acetonitrile were injected using an auto sampler (*12*).

Calculations and Statistical Analyses. After HPLC analysis, chromatograms were loaded and integrated. The integration results were exported as CSV files. One-way ANOVA followed by Tukey's test with adjusted α set at 0.05 was performed to compare data from all infected samples and all control samples; in addition, Student's *t*-test was applied to compare paired weekly data of infected and control samples. Peak alignment of HPLC chromatograms was achieved by retention time and UV characteristics, with missing values automatically set to zero. Before statistical analysis, relative amounts of the various compounds were obtained by normalizing peak area to 1 g of fresh plant tissue. The data set was exported for PCA analysis. Statistical analysis was performed using Origin 7.5 (OriginLab Inc., MA, USA). Principal component analysis (PCA) was performed using SIMCA-P 11 (Umetrics, UK).

Isolation of New Compounds. For isolation of new metabolites, infected roots (300 g fresh wt.) were harvested five weeks after inoculation. The roots were cut into small pieces, frozen in liquid nitrogen, and freeze-dried. The plant tissue was extracted with MeOH (3 × 1 L) with sonication, concentrated, and partitioned between H_2O-CH_2Cl_2. The CH_2Cl_2 layer (540 mg) was concentrated and fractionated by FCC (silica gel, EtOAc-hexane, 10:90 to 100:0) to yield 11 fractions (Fr.); Fr. 3 was purified by PTLC to yield **15** (1.0 mg), Fr. 4 and 5 were combined (8.3 mg) and purified by PTLC to yield **23** (2.1 mg), and Fr. 10 was further fractionated by PTLC on silica gel to yield **21** (2.2 mg). The aqueous layer containing polar metabolites was repeatedly fractionated on Diaion 101, Sephadex LH-20, and reverse phase silica gel (C18). A less polar fraction was further purified by PTLC to yield **37** (1.0 mg) and **38** (2.0 mg).

Antifungal Bioassays. *Rhizoctonia solani* AG 2-1, *Sclerotinia sclerotiorum*, and *Alternaria brassicicola* were obtained from Agricultural and Agri-Food Canada, Saskatoon, SK, Canada. Spores of *A. brassicicola*, sclerotia of *S. sclerotiorum*, and mycelia of *R. solani* were grown on potato dextrose agar (PDA) plates at 23 ± 2 °C under constant light. Solutions of compounds in DMSO were used to prepare sterile assay plates (6 wells per plate, 36 mm diameter, 2 mL per well) in PDA media (5.0×10^{-4} M, 2.5×10^{-4} M, 1×10^{-4} M; final DMSO concentration 1%). Control plates contained 1% DMSO in PDA. Plates containing test solutions and the control solution were inoculated with mycelia plugs (4 mm diameter) placed upside down on the center of each plate. The plates were incubated at 23 ± 2 °C under constant light for 24 h for *S. sclerotiorum*, 72 h for *R. solani*, and *A. brassicicola*. The radial growth of mycelia was measured and compared with control plates containing only DMSO. Each experiment was conducted in triplicate and repeated three times.

Synthesis of 4-Methoxycyclobrassinin (15). To a solution of 4-methoxybrassinin (17 mg, 0.06 mmol) in dry THF (3 mL) was added pyridinium bromide perbromide (PBP, 20 mg, 0.06 mmol). The reaction mixture was stirred at room temperature for 40 min. Then, the reaction mixture was basified with DBU (30 μL, 0.19 mmol), and the reaction was allowed to proceed for 1 h. After workup, the mixture was purified by FCC on silica gel to yield 4-methoxycyclobrassinin (**15**, 8.1 mg, 50% yield). EI-MS (*m/z*, relative abundance): 264 (16), 191 (100), 161 (16). HREI-MS (*m/z*, relative abundance): 264.0390, calc. 264.0391 for $C_{12}H_{12}N_2OS_2$. ESI-MS (positive, *m/z*, relative abundance): 265 (100), 217 (10), 192 (80). ^{1}H NMR (CD_3CN, 500 MHz): δ 9.32 (brs, 1H), 7.06 (t, J = 8.0 Hz, 1H), 6.98 (d, J = 8.0 Hz, 1H), 6.56 (d, J = 8.0 Hz, 1H), 5.48 (s, 2H), 3.93 (s, 3H), 2.54 (s, 3H). ^{13}C NMR (CD_3CN, 125.8 MHz): δ 153.3 (s), 151.2 (s), 138.3 (s), 122.7 (d), 119.8 (s), 104.4 (d), 102.9 (s), 100.2 (d), 54.9 (q), 49.7 (t), 14.5 (q).

Synthesis of Dehydrocyclobrassinin (17). Synthesis of dehydrocyclobrassinin was adapted from a previous procedure (*13*). 2,3-Dichloro-5,6-dicyano-1,4-benzoquinone (DDQ, 63 mg, 0.28 mmol) was added to a solution of cyclobrassinin (65 mg, 0.28 mmol) in benzene (5 mL). The reaction mixture was stirred at r.t. for 5 min. Then, the mixture was passed through a silica gel column and eluted with hexane-EtOAc (3:1) to yield dehydrocyclobrassinin (45 mg, 0.19 mmol, 70% yield). EI-MS (*m/z*, relative abundance): 232 (100), 199 (13), 159 (52). HREI-MS (*m/z*, relative abundance): 232.0134, calc. 232.0133 for $C_{11}H_8N_2S_2$. ^{1}H NMR ($CDCl_3$): δ 8.76 (s, 1H), 8.00 (d, J = 8.0 Hz, 1H), 7.77 (d, J = 8.0 Hz, 1H), 7.56 (t, J = 8.0 Hz, 1H), 7.36 (t, J = 8.0 Hz, 1H), 2.80 (s, 3H). ^{13}C NMR ($CDCl_3$): δ 170.1 (s), 157.8 (s), 152.9 (s), 139.2 (d), 129.5 (d), 124.2 (s), 123.3 (d), 120.5 (d), 119.0 (d), 118.6 (s), 15.2 (q).

Synthesis of 4-Methoxydehydrocyclobrassinin (18). Synthesis of 4-methoxydehydrocyclobrassinin was adapted from a previous procedure (*13*). 2,3-Dichloro-5,6-dicyano-1,4-benzoquinone (DDQ, 18 mg, 0.08 mmol) was added to a solution of 4-methoxycyclobrassinin (20.4 mg, 0.08 mmol) in benzene (5 mL). The reaction mixture was stirred at r.t. for 5 min. Then, the mixture was passed through a silica gel column and eluted with hexane-EtOAc (3:1) to yield 4-methoxydehydrocyclobrassinin (20 mg, 0.08 mmol, quantitative). EI-MS (*m/z*, relative abundance): 262 (100), 229 (14), 159 (12), 146 (13). HREI-MS (*m/z*, relative abundance): 262.0233, calc. 262.0234 for $C_{12}H_{10}N_2OS_2$. ^{1}H NMR ($CDCl_3$): δ 8.94 (s, 1H), 7.50 (t, J = 8.0 Hz, 1H), 7.40 (d, J = 8.0 Hz, 1H), 6.84 (d, J = 8.0 Hz, 1H), 4.07 (s, 3H), 2.79 (s, 3H). ^{13}C NMR ($CDCl_3$): δ 167.8 (s), 157.9 (s), 156.4 (s), 154.6 (s), 140.9 (d), 130.3 (d), 118.6 (s), 112.7 (s), 112.1 (d), 104.6 (d), 55.6 (q), 15.1 (q).

Synthesis of 3-Methylsulfonylmethylindole (21). A mixture of gramine (109 mg, 0.63 mmol) and sodium thiomethoxide (50 mg, 0.71 mmol) in H_2O (4 mL) was refluxed at 80 °C for 1 h. The reaction mixture was diluted with H_2O (20 mL) and extracted with Et_2O (3 × 20 mL). The combined organic solution was washed with 1N HCl (5 mL), dried over Na_2SO_4, and concentrated under reduced pressure. The residue was purified by FCC on silica gel (CH_2Cl_2) to yield 3-thiomethylmethylindole as white crystals (83 mg, 76% yield) (*14*). To a solution of thiomethylmethylindole (42 mg, 0.24 mmol)) in MeOH (1 mL) was added oxone (150 mg, 0.25 mmol) in H_2O (1 mL). The mixture was stirred at room temperature for 15 min. The mixture was diluted with H_2O (20 mL) and extracted with Et_2O (3 × 20 mL). The combined organic solution was dried over Na_2SO_4 and concentrated under reduced pressure. The residue was separated by FCC on silica gel (CH_2Cl_2) to yield 3-methylsulfonylmethylindole (29 mg, 58% yield) (*15*); yellow crystals, mp 154−155 °C. EI-MS (*m/z*, relative abundance): 209 (5), 130 (100), 102 (5), 77 (8). HREI-MS (*m/z*): 209.0506, calc. 209.0510 for $C_{11}H_{11}NSO_2$. CI-MS (positive, *m/z*, relative abundance): 227 (100), 168 (10), 130 (94). ESI-MS (positive, *m/z*, relative abundance): 232 $[M + Na]^+$ (10), 210 (1), 130 (100). ^{1}H NMR (500.3 MHz, in $CDCl_3$): δ 8.48 (brs, 1H), 7.67 (d, J = 8 Hz, 1H), 7.45 (d, J = 8 Hz, 1H), 7.39 (d, J = 2.5 Hz, 1H), 7.28 (t, J = 8 Hz, 1H), 7.24 (t, J = 8 Hz, 1H), 4.50 (s, 2H), 2.77 (s, 3H). ^{13}C NMR (125.8 MHz, in $CDCl_3$): δ 136.0 (s), 126.6 (s), 125.8 (d), 122.9 (d), 120.8 (d), 118.3 (d), 111.7 (d), 102.9 (s), 52.6 (t), 38.9 (q). UV (MeOH) λ_{max} (nm): 217 (log ε, 4.54), 278 (log ε, 3.76), 288 (log ε, 3.68). FTIR (KBr) υ_{max} (cm^{-1}): 2924, 2852, 1611, 1383, 1113, 1027.

Synthesis of 1-Methoxy-3-methoxymethylindole (23). Sodium hydride (28 mg, 0.69 mmol) was added to a solution of 1-methoxyindole-3-methanol (*16*) (40.4 mg, 0.23 mmol) in THF (2 mL) with stirring. Iodomethane (22 μL, 0.35 mmol) was added to the mixture. The reaction was stirred at r. t. for 1 h. Then, the reaction was quenched with water (10 mL). The mixture was extracted with Et_2O (3 × 20 mL), and the organic layer was dried over Na_2SO_4 and concentrated under reduced pressure. The crude material was separated by FCC to yield 1-methoxy-3-methoxymethylindole (**23**) as a white oil (27.4 mg, 65% yield). HREI-MS (*m/z*, relative abundance): 191.0699, calc. 191.0768 for $C_{11}H_{11}NO_2$. ESI-MS (positive, *m/z*, relative abundance): 192 (5), 176 (6), 160 (100), 145 (95). ^{1}H NMR (500.3 MHz, $CDCl_3$):

δ 7.70 (d, J = 8 Hz, 1H), 7.45 (d, J = 8 Hz, 1H), 7.30 (s, 1H), 7.28 (t, J = 8 Hz, 1H), 7.17 (t, J = 8 Hz, 1H), 4.65 (s, 2H), 4.11 (s, 3H), 3.43 (s, 1H). ^{1}H NMR (500.3 MHz, CD_3CN): δ 7.66 (d, J = 8 Hz, 1H), 7.47 (d, J = 8 Hz, 1H), 7.43 (s, 1H), 7.28 (t, J = 8 Hz, 1H), 7.15 (t, J = 8 Hz, 1H), 4.60 (s, 2H), 4.10 (s, 3H), 3.33 (s, 1H). ^{13}C NMR (125.8 MHz, CD_3CN): δ 56.6 (q), 65.6 (q), 65.7 (t), 108.3 (d), 109.0 (s), 119.4 (d), 119.9 (d), 122.5 (d), 122.9 (d), 123.6 (s), 132.4 (s). UV (CH_2Cl_2) λ_{max} (nm): 227 (log ε, 4.31), 277 (log ε, 3.79).

Synthesis of Dihydroascorbigen (37) and Dihydroneoascorbigen (38). To a solution of ascorbigens in MeOH was added $NaBH_4$ in small portions. The mixture was stirred at room temperature for 10 min, the solvent was removed, and the residue was purified by FCC on silica gel (CH_2Cl_2: MeOH, 10:1) to obtain a pure product (*17*).

*Dihydroascorbigen (***37***).* EI-MS (*m/z*, relative abundance): 307 (9), 130 (100). HREI-MS (*m/z*, relative abundance): 307.1055, calc. 307.1055 for $C_{15}H_{17}NO_6$. ESI-MS (positive, *m/z*, relative abundance): 308.1 (100), 262.3 (30), 130.3 (10). $[\alpha]_D$ +22 (*c* 0.7, MeOH). ^{1}H NMR (500.3 MHz, in D_2O): δ 7.53 (d, J = 8 Hz, 1H), 7.40 (d, J = 8 Hz, 1H), 7.21 (s, 1H), 7.13 (t, J = 8 Hz, 1H), 7.03 (t, J = 8 Hz, 1H), 4.45 (d, J = 8.5 Hz, 1H), 4.02 (d, J = 7.5 Hz, 1H), 3.75 (m, 1H), 3.52 (d, J = 6 Hz, 2H), 3.36 (d, J = 14.5 Hz, 1H), 3.18 (d, J = 14.5 Hz, 1H). ^{13}C NMR (125.8 MHz, in D_2O): δ 26.9 (t), 61.7 (t), 68.7 (d), 74.3 (d), 78.3 (s), 80.0 (s), 106.0 (s), 111.1 (d), 118.1 (d), 118.6 (d), 121.0 (d), 125.6 (d), 127.0 (s), 135.5 (s), 178.1 (s). UV (MeOH) λ_{max} (nm): 220 (log ε, 4.37), 281 (log ε, 3.62), 290 (log ε, 3.54). FTIR (KBr) υ_{max} (cm^{-1}): 3355, 2919, 2852, 1643, 1606, 1513, 1385, 1140, 812.

*Dihydroneoascorbigen (***38***).* EI-MS (*m/z*, relative abundance): 337 (11), 160 (100). HREI-MS (*m/z*, relative abundance): 337.1160, calc. 337.1161 for $C_{16}H_{18}NO_7$. $[\alpha]_D$ +16 (*c* 0.5, MeOH). ^{1}H NMR (500.3 MHz, in D_2O): δ 7.53 (d, J = 8 Hz, 1H), 7.43 (d, J = 8 Hz, 1H), 7.35 (s, 1H), 7.21 (t, J = 8 Hz, 1H), 7.06 (t, J = 8 Hz, 1H), 4.45 (d, J = 8.5 Hz, 1H), 4.02 (d, J = 7.5 Hz, 1H), 3.98 (s, 3H), 3.75 (m, 1H), 3.52 (m, 2H), 3.31 (d, J = 14.5 Hz, 1H), 3.14 (d, J = 14.5 Hz, 1H). ^{13}C NMR (125.8 MHz, in D_2O): δ 26.9 (t), 61.9 (t), 65.9 (q), 68.9 (d), 74.4 (d), 78.4 (s), 80.2 (s), 108.5 (s), 111.1 (d), 118.9 (d), 119.6 (d), 122.6 (d), 123.9 (s), 124.2 (d), 131.6 (s), 178.0 (s). UV (MeOH) λ_{max} (nm): 222 (log ε, 4.27), 290 (log ε, 3.51). FTIR (KBr) υ_{max} (cm^{-1}): 3297, 2958, 2867, 1646, 1602, 1513, 1385, 1141, 834.

RESULTS

One-week-old seedling roots of canola (*B. napus* cv. Westar) were infected with a suspension of spores of *P. brassicae* as described in Materials and Methods. Seedlings were transferred to pots, incubated, and harvested as described above. Extraction of the pulverized roots provided the nonpolar (NP) extracts, whereas the remaining residues provided the polar (PP) extracts, all of which were analyzed by HPLC-DAD and HPLC-ESI-MS. Examples of each chromatogram are shown in **Figures 1**−**4**. The identity of each metabolite was established either by direct comparison of authentic samples available in our metabolite libraries (HPLC-DAD and HPLC-ESI-MS; **1**, **2**, **9**, **11**, **16**, and **30**) or by isolation and structure determination using NMR and MS spectroscopic data (**3**−**8**, **10**, **12**−**15**, **17**−**29**, and **31**−**45**). The structural assignments of all new metabolites **15**, **17**, **21**, **23**, **37**, and **38** by spectroscopic methods were confirmed by the chemical synthesis of each compound, as described in Materials and Methods.

Qualitative and Quantitative Analysis of Nonpolar Extracts. Twenty-nine metabolites (**1**−**29**) were identified from nonpolar extracts of the roots of canola infected with *P. brassicae* (**Figures 5** and **6**). Phytoalexins were detected in infected roots only three weeks after inoculation; however, a higher number of phytoalexins were detected five and six weeks after inoculation: brassicanal A (**1**), caulilexin A (**2**), spirobrassinin (**3**), brassilexin (**4**), brassicanate A (**9**), brassinin (**11**), 4-methoxybrassinin (**12**), cyclobrassinin (**13**), 1-methoxybrassinin (**14**), 4-methoxycyclobrassinin (**15**), sinalbin B (**16**), dehydrocyclobrassinin (**17**), and 4-methoxydehydrocyclobrassinin (**18**). No phytoalexins were detected in the leaves of canola whose roots were infected with *P. brassicae* at any point of the infection. A number of indolyl metabolites were present in both infected and control roots, including indolyl-3-acetonitrile (**5**), arvelexin (**6**), caulilexin C (**7**), ascorbigen (**19**), neoascorbigen (**20**), 3-methylsulfonylmethylindole (**21**), 1-methoxyindole-3-methanol (**22**), 1-methoxy-3-methoxymethylindole (**23**), indole-3-carboxaldehyde (**24**), 4-methoxyindole-3-carboxaldehyde (**25**),

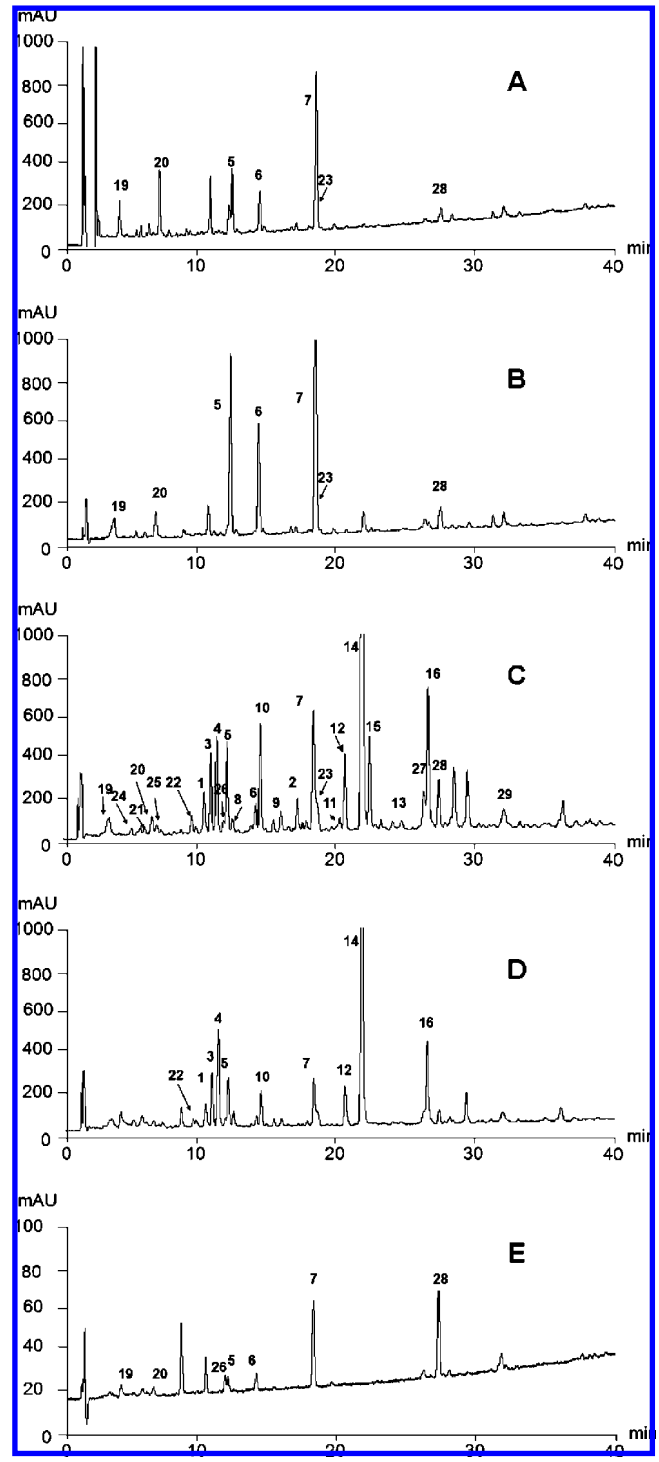

Figure 1. HPLC-DAD chromatograms of nonpolar extracts of canola (*Brassica napus* cv. Westar) roots infected with *Plasmodiophora brassicae*; **A**, 3-weeks post-inoculation; **B**, 4-weeks post-inoculation; **C**, 5-weeks post-inoculation; **D**, 6-weeks post-inoculation; **E**, 5-weeks control. Conditions as reported in Materials and Methods.

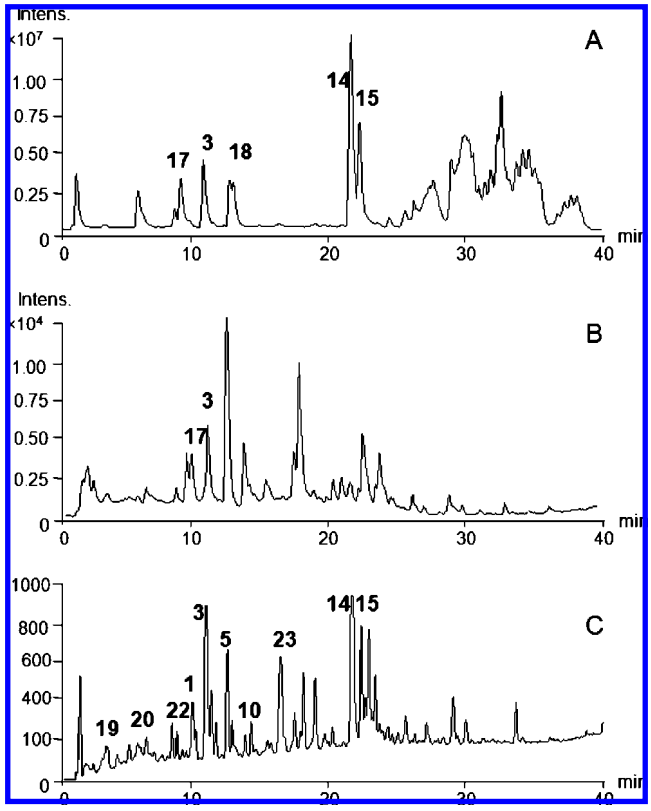

Figure 2. HPLC-DAD-ESI chromatograms of nonpolar extracts of canola (*Brassica napus* cv. Westar) roots 5-weeks postinoculation with *Plasmodiophora brassicae*; **A**, ESI positive mode; **B**, ESI negative mode; **C**, DAD. Conditions as reported in Materials and Methods.

1-methoxyindole-3-carboxaldehyde (**26**), and di-indoles **27**, **28**, and **29**. Although indolyl-3-acetonitrile (**5**), arvelexin (**6**), and caulilexin C (**7**) were previously found to be phytoalexins (*2*), in this work, they were found also in control samples; thus, these metabolites are not phytoalexins in canola (*B. napus*). The metabolites 3-methylsulfonylmethylindole (**21**) and 1-methoxy-3-methoxymethylindole (**23**) as well as the cyclobrassinins **15** and **17** are reported here for the first time as naturally occurring metabolites. The identification, synthesis, and bioactivity of these new metabolites (**15**, **17**, **21**, and **23**) from nonpolar extracts are described below.

Quantitative analysis of metabolites obtained in nonpolar extracts was achieved using HPLC-DAD analysis (NP method) and calibration curves built for each compound using purified samples. Only metabolites present in reasonable concentrations were quantified (>0.1 nmol/g fresh weight). Statistical analysis was performed as described in Materials and Methods. Quantitative analysis of the phytoalexins spirobrassinin (**3**), brassilexin (**4**), brassicanate A (**9**), rutalexin (**10**), 4-methoxybrassinin (**12**), and cyclobrassinin (**13**) showed that cyclobrassinin was produced in significantly larger amounts than any other phytoalexins (**Figure 7**). Spirobrassinin (**3**, 21−26 nmol/g fresh wt) and brassilexin (**4**, 5−7 nmol/g fresh wt) were detected only in samples collected five and six weeks after inoculation. Rutalexin (**10**) was present in roots collected four weeks after inoculation in low concentration, but in significantly higher concentration in roots collected five and six weeks after inoculation (9.6 and 8.5 nmol/g fresh wt., respectively). Brassicanate A (**9**), 4-methoxybrassinin (**12**), and cyclobrassinin (**13**) were present in roots collected three weeks after inoculation and thereafter. However, brassicanate A (**9**) appeared to be produced in much lower amounts than **12** or **13**, which were produced in significantly

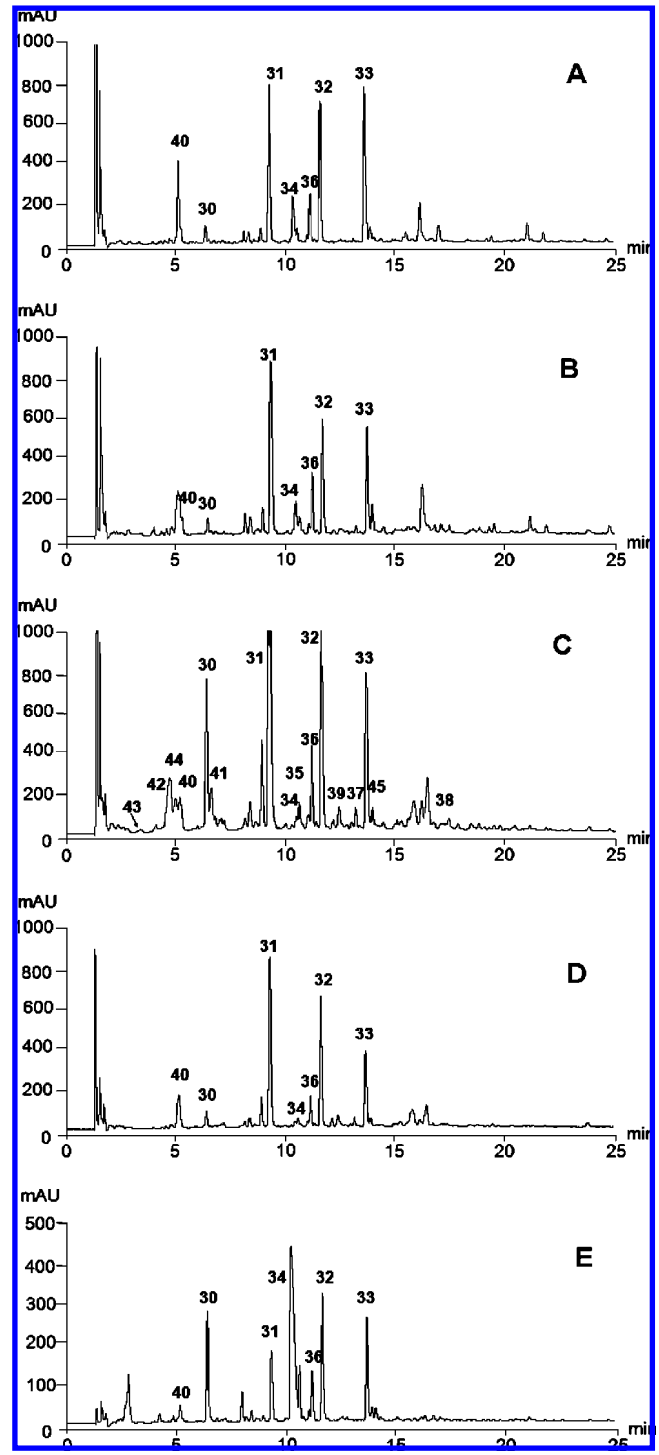

Figure 3. HPLC-DAD chromatograms of polar extracts of canola (*Brassica napus* cv. Westar) roots infected with *Plasmodiophora brassicae*; **A**, 3-weeks post-inoculation; **B**. 4-weeks post-inoculation; **C**, 5-weeks post-inoculation; **D**, 6-weeks post-inoculation; **E**, 5-weeks control. Conditions as reported in Materials and Methods.

higher concentrations in roots collected five and six weeks after inoculation. The concentration of 4-methoxybrassinin (**12**) was about 32 nmol/g fresh wt. at later stages, while cyclobrassinin (**13**) was induced in much higher concentrations, 120−160 nmol/g fresh wt.

Other quantifiable metabolites present in the nonpolar extracts of both control and infected roots included indolyl-3-acetonitrile (**5**), arvelexin (**6**), caulilexin C (**7**), ascorbigen (**19**), and neoascorbigen (**20**) (**Figure 8**). Compared with control samples,

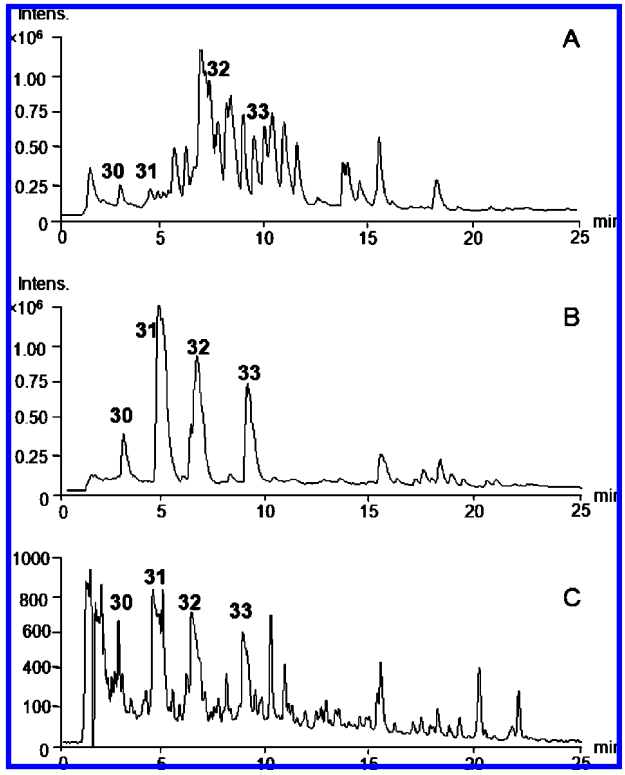

Figure 4. HPLC-DAD-ESI chromatograms of polar extracts of canola (*Brassica napus* cv. Westar) roots 5-week post-inoculation with *Plasmodiophora brassicae*; **A**, ESI positive mode; **B**, ESI negative mode; **C**, DAD. Conditions as reported in Materials and Methods.

the concentration of indolyl-3-acetonitrile (**5**) was significantly higher in infected roots collected three and four weeks after inoculation ($P < 0.05$). The highest concentration of indolyl-3-acetonitrile (**5**) in infected roots was detected four weeks after inoculation (31.4 nmol/g fresh wt.); at later stages, there were no differences in infected and control samples (**Figure 8**). Similarly, relative to controls the concentration of arvelexin (**6**) increased significantly three and four weeks after inoculation ($P < 0.01$) (**Figure 8**). By contrast, the concentration of caulilexin C (**7**) was significantly higher than that of control roots three weeks after inoculation ($P < 0.01$) (**Figure 8**). Relative to control samples, the concentration of ascorbigen (**19**) was significantly higher in infected roots collected three weeks after inoculation (59.3 nmol/g fresh wt., $P < 0.05$) (**Figure 8**). Similarly, the concentration of neoascorbigen (**20**) was significantly higher than that of control samples in roots collected three weeks after inoculation (46.4 nmol/g fresh wt., $P < 0.05$) (**Figure 8**).

Qualitative and Quantitative Analysis of Polar Extracts. Sixteen metabolites (**30**−**45**) were identified from polar extracts of roots of *B. napus* infected with *P. brassicae* (**Figures 3** and **4**). These metabolites were detected both in infected and control roots: 4-hydroxyglucobrassicin (**30**), glucobrassicin (**31**), 4-methoxyglucobrassicin (**32**), neoglucobrassicin (**33**), gluconasturtiin (**34**), coniferin (**35**), syringin (**36**), dihydroascorbigen (**37**), dihydroneoascorbigen (**38**), roseoside (**39**), adenine (**40**), adenosine (**41**), uridine (**42**), tyrosine (**43**), cytidine (**44**), and tryptophan (**45**) (**Figure 6**). Among these metabolites, dihydroascorbigen (**37**) and dihydroneoascorbigen (**38**) are new metabolites whose structures were determined as described below.

Quantitative analysis of metabolites obtained in polar extracts was achieved using HPLC-DAD analysis (PP method) and calibration curves built for each compound using purified samples. Only metabolites present in reasonable concentrations were quantified (>0.1 nmol/g fresh weight). Statistical analysis was performed as described in Materials and Methods. The major components of the polar extracts included indolyl glucosinolates **30**−**33**, aromatic glucosinolate **34**, and phenylpropanoids **35** and **36**. Root samples collected three and four weeks after inoculation contained indolyl glucosinolates **30**−**33** in concentrations similar to those of controls. The concentration of 4-methoxyglucobrassicin (**32**) was significantly lower in infected roots than in control roots five weeks after inoculation (ANOVA and Student's *t*-test). However, the concentrations of **31** and **33** in infected roots five and six weeks after inoculation were not significantly different from same age control roots (ANOVA). In addition, roots collected five and six weeks after inoculation contained gluconasturtiin (**34**), coniferin (**35**), and syringin (**36**) in significantly lower concentrations than control roots (**Figure 9**).

Identification of 4-Methoxycyclobrassinin (15). The HPLC chromatograms (DAD and LC-ESI-MS) of nonpolar extracts of roots infected with *P. brassicae* five weeks after inoculation showed a peak at $t_R = 22.0$ min with spectral characteristics similar to those of 1-methoxycyclobrassinin (**16**, $t_R = 33$ min); however, its retention time indicated that it was not **16**. This metabolite displayed fragments similar to those observed for **16** in ESI-MS positive ion mode, including 265 $[M + 1]^+$ (100%), 217 $[M\text{-}SCH_3]^+$ (10%), and 192 (80%) (**Table 1**). For this reason, the structure of the peak with $t_R = 22.0$ min was proposed to be 4-methoxycyclobrassinin (**15**). Further confirmation of its occurrence *in planta* was achieved after its isolation from infected roots (ca. 1 mg from 300 g infected roots). The ^{1}H NMR spectral data of the isolated sample was identical to those of the synthetic sample, prepared as described in Materials and Methods. 4-Methoxycyclobrassinin (**15**) has not been reported from plants, though it was previously synthesized by Monde et al. (*13*).

Dehydrocyclobrassinin (17) and 4-Methoxydehydrocyclobrassinin (18). The HPLC chromatograms (LC-ESI-MS, positive mode) of nonpolar extracts of roots infected with *P. brassicae* five weeks after inoculation showed peaks at $t_R =$ 11.0 (*m*/*z* 233) and 14.0 (*m*/*z* 263), which were not detected in control roots (**Figure 2**) and not available in our metabolite library (*12*). Considering that cyclobrassinin (**14**) and 4-methoxycyclobrassinin (**15**) were detected under the same conditions and that the unidentified compounds were 2 amu lower than the corresponding cyclobrassinins **14** and **15**, dehydrocyclobrassinin (**17**) and 4-methoxydehydrocyclobrassinin (**18**) were proposed to be responsible for peaks at $t_R = 11.0$ and 14.0 min, respectively. These structures were confirmed after the synthesis of each metabolite by oxidation of the corresponding cyclobrassinins using DDQ, as reported in Materials and Methods.

3-Methylsulfonylmethylindole (21). Compound **21** was isolated from nonpolar extracts as an amorphous powder. HPLC analysis indicated it to be another indole derivative not available in our library. ^{1}H NMR showed, apart from the indole ring, a methylene group (δ 4.50 ppm) and a rather deshielded methyl group (δ 2.79 ppm), consistent with a methylsulfone. The metabolite did not show diagnostic fragments in ESI-MS but in CI-MS showed ions at *m*/*z* 227 $[M + NH_4]^+$, 209, and 130. To accommodate these spectral characteristics, structure **21** was proposed and further confirmed by synthesis, as described in Materials and Methods.

1-Methoxy-3-methoxymethylindole (23). The HPLC chromatograms (DAD) of nonpolar extracts of infected roots four

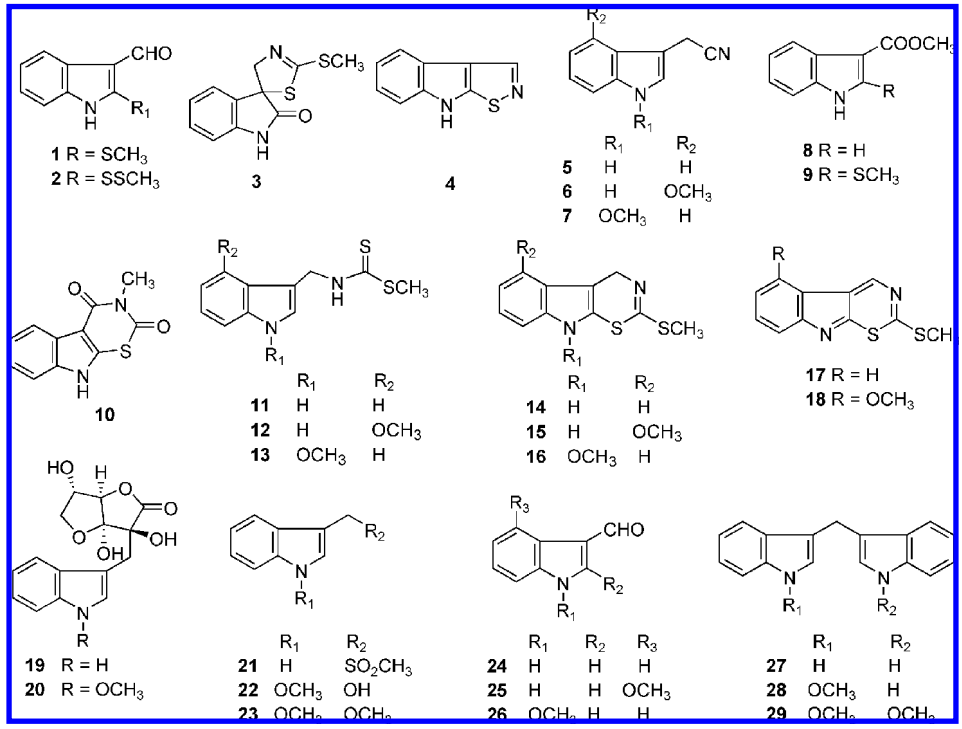

Figure 5. Chemical structures of metabolites detected in nonpolar (NP) extracts of roots of canola (*Brassica napus* cv. Westar) infected with *Plasmodiophora brassicae*; **1**, brassicanal A; **2**, caulilexin A; **3**, spirobrassinin; **4**, brassilexin; **5**, indolyl-3-acetonitrile; **6**, arvelexin; **7**, caulilexin C; **8**, methyl indole-3-carboxylate; **9**, brassicanate A; **10**, rutalexin; **11**, brassinin; **12**, 4-methoxybrassinin; **13**, 1-methoxybrassinin; **14**, cyclobrassinin; **15**, 4-methoxycyclobrassinin; **16**, sinalbin B; **17**, dehydrocyclobrassinin; **18**, 4-methoxydehydrocyclobrassinin; **19**, ascorbigen; **20**, neoascorbigen; **21**, 3-methylsulfonylmethylindole; **22**, 1-methoxyindole-3-methanol; **23**, 1-methoxy-3-methoxymethylindole; **24**, indole-3-carboxaldehyde; **25**, 4-methoxyindole-3-carboxaldehyde; **26**, 1-methoxy indole-3-carboxaldehyde; **27**−**29**, diindolylmethanes.

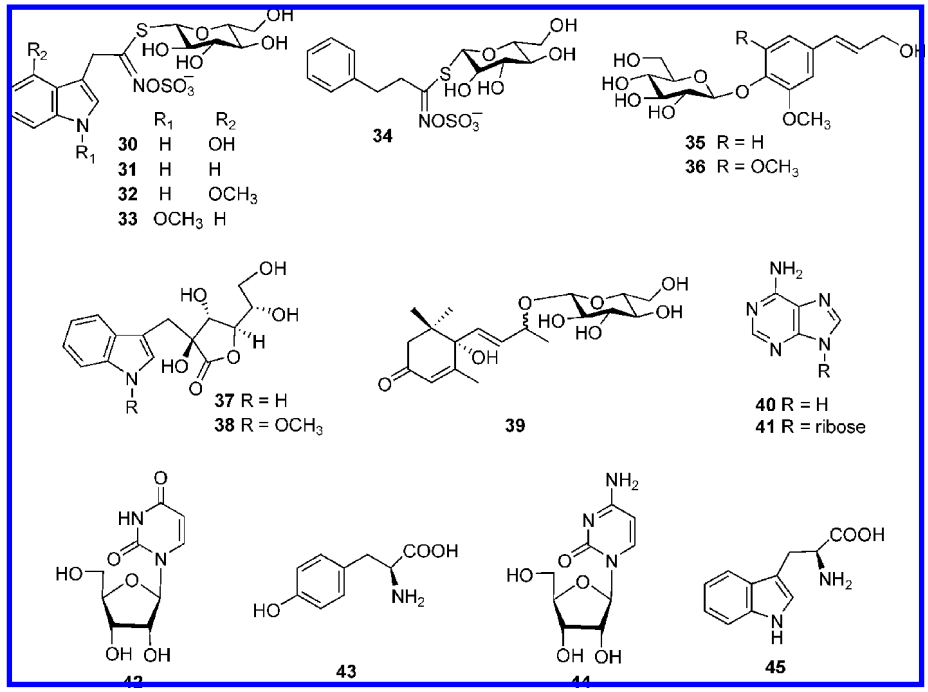

Figure 6. Chemical structures of metabolites detected in polar (PP) extracts of roots of canola (*Brassica napus* cv. Westar) infected with *Plasmodiophora brassicae*; **30**, 4-hydroxyglucobrassicin; **31**, glucobrassicin; **32**, 4-methoxyglucobrassicin; **33**, neoglucobrassicin; **34**, gluconasturtiin; **35**, coniferin; **36**, syringin; **37**, dihydroascorbigen; **38**, dihydroneoascorbigen; **39**, roseoside; **40**, adenine; **41**, adenosine; **42**, uridine; **43**, tyrosine; **44**, cytidine; **45**, tryptophan.

to six weeks after inoculation with *P. brassicae* showed a shoulder adjacent to the peak of caulilexin C (**7**, $t_R = 17.9$ min) whose spectral characteristics appeared to be different from those of known phytoalexins (**Figure 1**). Further confirmation of its occurrence *in planta* was obtained after its isolation from infected roots (ca. 3 mg from 300 g infected roots). HR-EI-MS spectral data of this isolated material suggested the molecular formula $C_{11}H_{13}NO_2$ (*m*/*z* 191.0699). The ^{1}H NMR spectral data displayed, apart from the five protons characteristic of a 3-substituted indole, two methoxy groups and two methylene

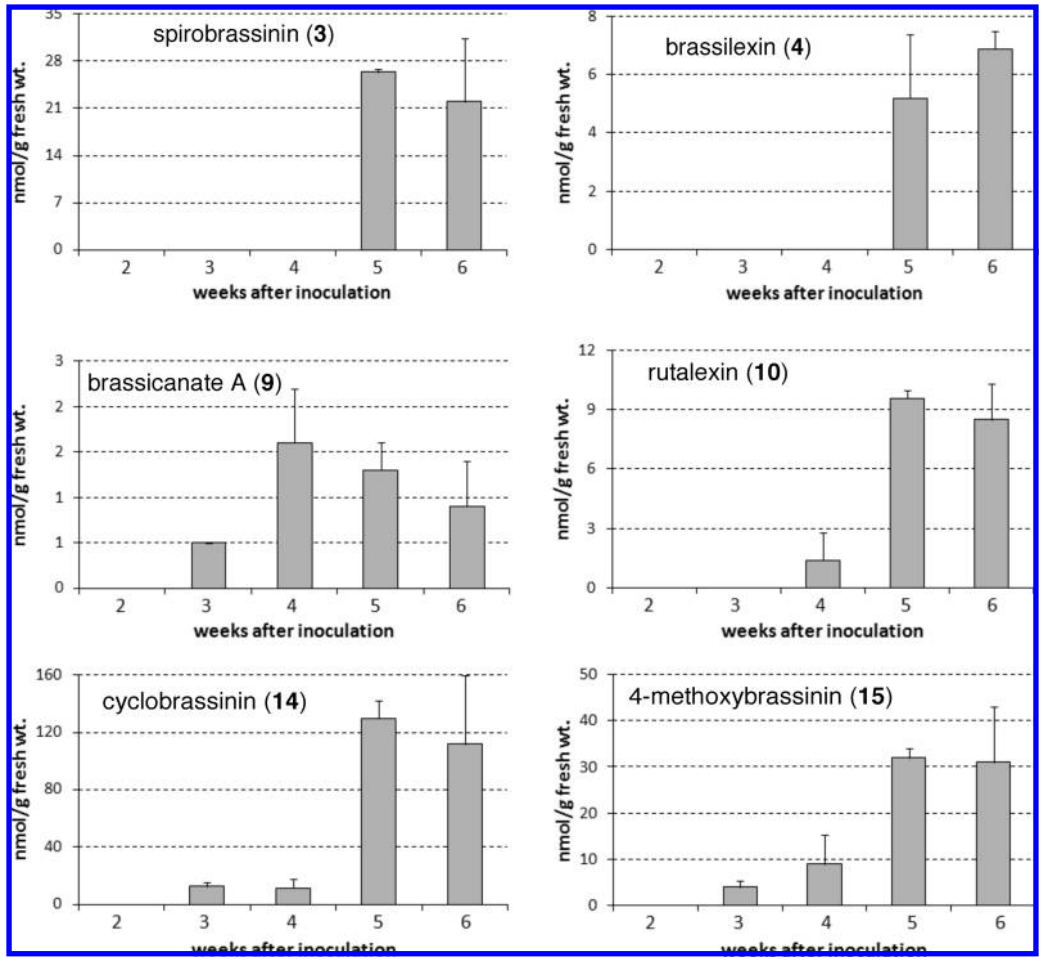

Figure 7. Accumulation of phytoalexins in roots of canola (*Brassica napus* cv. Westar) infected with *Plasmodiophora brassicae* over a six-week period. HPLC analysis is as described in Materials and Methods.

protons resonating at δ 4.65 ppm. The absence of the NH proton suggested that a methoxy group was located at N-1 of the indole and that the second methoxy group was likely attached to the methylene group. Therefore, metabolite **23** was proposed to be 1-methoxy-3-methoxymethylindole. The ^{1}H NMR spectral data of the isolated sample was identical to those of the synthetic sample, prepared as described in Materials and Methods.

Dihydroascorbigen (37) and Dihydroneoascorbigen (38). Compounds **37** and **38** were isolated from the polar extract as an amorphous powder. HPLC analysis indicated them to be indole derivatives not available in our library. The ^{1}H NMR of compound **37** showed resonances similar to those of ascorbigen except for an additional proton at δ 4.45 ppm and the signals of H_2-6′ (δ 3.51, J = 6.5 Hz, d, 2 H), which in ascorbigen were well separated at δ 4.99 (J = 11.0 Hz, d) and δ 4.05 (J = 4.5, 11.0 Hz, dd). ESI-MS spectral data showed a likely molecular ion at m/z 308, that is, 2 amu higher than the $[M + 1]^+$ of ascorbigen (**19**). This data indicated that the hemiacetal ring of ascorbigen (**19**) had been reduced to yield new metabolite **37**. HMBC spectral data showed that the additional proton at δ 4.45 was attached to C-3′ since it showed correlations with C-1′, C-CH_2, and C-5′. Its coupling constant (J = 8.5 Hz) indicated a *trans* stereochemistry relative to H-4′. Therefore, compound **37** was proposed to be dihydroascorbigen. The ^{1}H NMR signals of **38** were similar to those of dihydroascorbigen (**37**) except for an additional methoxy group (δ 3.98 ppm). Since both compounds showed similar proton signals for the sugar moiety as well as the indole skeleton, the methoxy group had to be attached to N-1. Therefore, compound **38** was proposed to be dihydroneoascorbigen. For further confirmation of the structures, compounds **37** and **38** were prepared by reduction of ascorbigen (**19**) and neoascorbigen (**20**), respectively. The spectra of the synthetic samples were identical to those of the isolated samples.

Multivariate analysis. Samples were prepared and analyzed as described in Materials and Methods. After analysis, the data set was exported into SIMCA-P for principal component analysis (PCA) (Data set in Supporting Information). The absolute quantities of each metabolite were calculated from peak areas and calibration curves. Principal component analysis (PCA) using the absolute quantities of 17 metabolites obtained from analyses of the roots of *B. napus* infected with *P. brassicae* was performed (**Figures 10** and **11**; data set in Supporting Information). This group of 17 metabolites included 11 nonpolar metabolites [indolyl-3-acetonitrile (**5**), arvelexin (**6**), caulilexin C (**7**), ascorbigen (**19**), neoascorbigen (**20**), spirobrassinin (**3**), brassilexin (**4**), rutalexin (**5**), brassicanate A (**9**), 4-methoxybrassinin (**12**), and cyclobrassinin (**13**)] and 6 polar metabolites [glucobrassicin (**31**), 4-methoxyglucobrassicin (**32**), neoglucobrassicin (**33**), gluconasturtiin (**34**), syringin (**36**), and coniferin (**35**)]. The PCA score plot (**Figure 10**) indicated a cluster of three groups; the first group included roots harvested two, three, and four weeks after inoculation with *P. brassicae*, which were very close to most of the control samples harvested at similar times (two, three, and four weeks after planting). By contrast, roots harvested five and six weeks after inoculation with *P. brassicae* were different from the first group and from control samples collected at the same time. Furthermore, the PCA

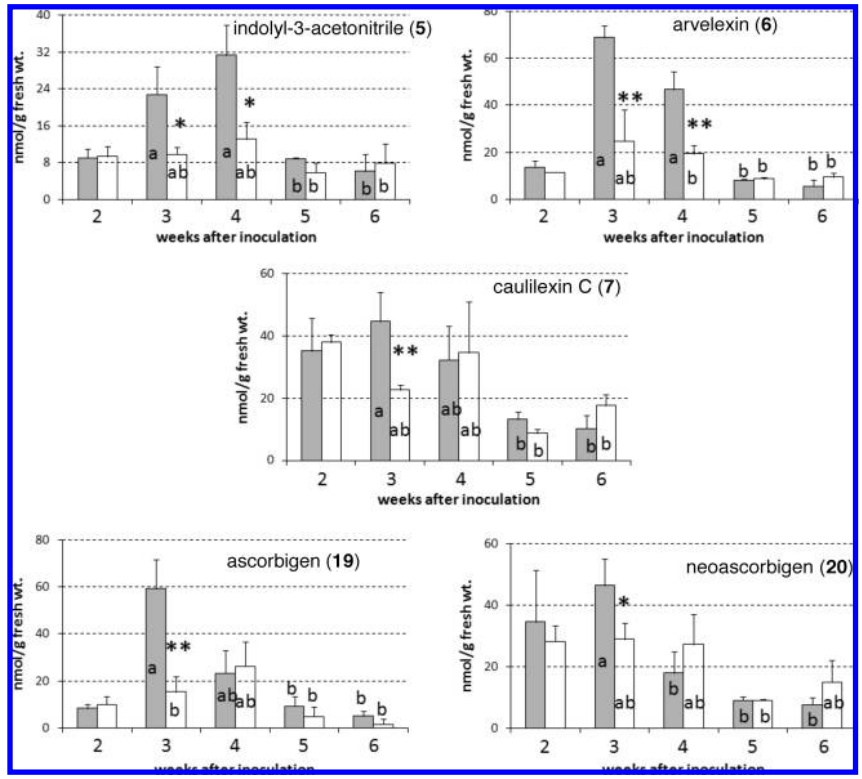

Figure 8. Accumulation of nonpolar (NP) metabolites in roots of canola (*Brassica napus* cv. Westar) infected with *Plasmodiophora brassicae* over a six-week period. HPLC analysis is as described in Materials and Methods. Gray bars, infected roots; open bars, control roots. For statistical analysis, one-way ANOVA tests were performed followed by Tukey's test with adjusted α set at 0.05; $n = 3$; error bar, standard deviation (same letters indicate nonsignificant differences); Student's *t*-test, * $P < 0.05$; ** $P < 0.01$.

loading plot separated all 17 compounds into three different groups (**Figure 11**). All phytoalexins (**3**, **4**, **10**, **9**, **12**, and **13**) were set into one group, while indolyl-3-acetonitriles (**5**, **6**, and **7**) and ascorbigens (**19** and **20**) were set into another group, with the third group including the more polar metabolites [indolyl glucosinolates **31**, **32**, **33**, gluconasturtiin (**34**), and phenylpropanoids coniferin (**35**) and syringin (**36**)].

Next, PCA analysis of a more complex data set that included the relative amount of 107 metabolites detected by HPLC-DAD analysis of the roots of canola infected with *P. brassicae* (data set in Supporting Information) was performed. The two component PCA model (PC1 vs PC2) successfully discriminated among tested samples (**Figure 12**). Furthermore, triplicate samples were closely related in the score plot indicating the reproducibility of experiments (**Figure 12**). The score plot showed discrimination among three groups by principal components PC1 and PC2. Group I contains both control samples and infected samples two weeks after inoculation and planting, indicating that the metabolic profiles in controls and infected roots were similar. Roots harvested three and four weeks after inoculation were slightly different from control roots and were clustered into group II, whereas roots harvested five and six weeks after inoculation were set into group III, which showed a significantly different metabolite content from any other roots.

Antifungal Assays. The antifungal activity of metabolites **15**, **17**−**21**, **23**, **26**, **37**, and **38** against three important pathogens of canola (*Rhizoctonia solani*, *Alternaria brassicicola*, and *Sclerotinia sclerotiorum*) was investigated using the mycelia radial growth bioassay described in Materials and Methods (**Table 2**). *P. brassicae* is not amenable to aseptic culture and thus cannot be tested under similar conditions. 4-Methoxycyclobrassinin (**15**) showed the highest inhibitory effect against *S. sclerotiorum* at 0.50 mM, a milder effect against *R. solani*, and no inhibitory effect against *A. brassicicola*. Dehydrocyclobrassinin (**17**) and 4-methoxydehydrocyclobrassinin (**18**) showed a moderate inhibitory effect against *S. sclerotiorum* at 0.50 mM, but a stronger effect against *R. solani*, and no inhibitory effect against *A. brassicicola*. Ascorbigen (**19**) and neoascorbigen (**20**) showed mild inhibition of *R. solani* and *S. sclerotiorum*, while no inhibition effect against *A. brassicicola* was observed. 1-Methoxyindole-3-carboxaldehyde (**26**) and 1-methoxy-3-methoxymethylindole (**23**) showed mild growth inhibition against *R. solani*, *A. brassicicola*, and *S. sclerotiorum*. 3-Methylsulfonylmethylindole (**21**) showed mild inhibitory effect against *S. sclerotiorum*, while no inhibitory effect was observed against *R. solani* and *A. brassicicola*. Dihydroascorbigen (**37**) showed stronger inhibitory effect against *R. solani* than dihydroneoascorbigen (**38**), while no inhibitory effect was observed against *A. brassicicola*. Both metabolites **37** and **38** showed mild activity against *S. sclerotiorum*.

DISCUSSION

The work reported above revealed for the first time that roots of canola (*B. napus* cv. Westar) under biotrophic attack produced both phytoalexins and phytoanticipins, some of which were previously unknown (**Figures 1** and **3**). 4-Methoxycyclobrassinin (**15**) and dehydrocyclobrassinin (**17**), reported here for the first time to be produced in a plant, are induced in response to pathogen infection and display antifungal activity, thus are two new crucifer phytoalexins. Other new metabolites that showed mild antifungal activity, 3-methylsulfonylmethylindole (**21**), 1-methoxy-3-methoxymethylindole (**23**), dihydroascorbigen (**37**), and dihydroneoascorbigen (**38**), are classified as new phytoanticipins since they were produced both in infected and

Table 1. Characterization of Metabolites **1**−**45** from the Roots of *Brassica napus* Using HPLC-DAD-ESI-MS Analyses

compound	t_R (min)	F.W.	positive mode MS (relative abundance)	negative mode MS (relative abundance)	UV λ_{max} (nm)
			Nonpolar Metabolites[a]		
ascorbigen (**19**)	3.1	305	306 (70), 130 (100)	ND[c]	200, 220, 281, 288
indole-3-carboxaldehyde (**24**)	5.4	145	168 $[M + Na]^+$ (5), 146 (70), 118 (100)	144 (100)	210, 245, 260, 300
methylsulfonylmethylindole (**21**)	6.5	209	232$[M + Na]^+$ (10), 210 (1), 130 (100)	ND[c]	217, 278, 288
neoascorbigen (**20**)	6.6	335	336 (100), 304 (40), 160 (20), 130 (8)	669 (100)	220, 290
4-methoxyindole-3-carboxaldehyde (**25**)	7.6	175	198$[M + Na]^+$ (13), 176 (100), 161 (7), 148 (9)	174 (100), 160 (41)	220, 260, 289
1-methoxyindole-3-methanol (**22**)	9.1	175	392 (100), 176 (5), 160 (66), 146 (68)	390 (100), 144 (20)	200, 220, 270, 286
brassicanal a (**1**)	9.3	191	214 $[M + Na]^+$ (6), 192 (100), 164 (14), 117 (24)	190 (100), 175 (9)	218, 258, 269, 325
dehydrocyclobrassinin (**17**)	10.1	232	233 (100)	ND[c]	210, 250, 270, 360
indolyl-3-acetonitrile (**5**)	10.6	156	179 $[M + Na]^+$ (2), 157 (5), 130 (100)	ND[c]	220, 272, 285
brassilexin (**4**)	10.7	174	175 (100), 148 (8)	173 (100)	220, 245, 264
spirobrassinin (**3**)	10.9	250	273 $[M + Na]^+$ (8), 251 (100), 203 (21), 178 (8)	249 (89), 217 (3), 201 (100)	220, 258, 296
1-methoxy indole-3-carboxaldehyde (**26**)	11.8	175	198$[M + Na]^+$ (2), 176 (100), 161 (23), 133 (40)	199 (10), 175 (13), 165 (80), 145 (100)	210, 248, 298
methyl indole-3-carboxylate (**8**)	12.1	175	145 (100)	174 (100)	218, 228, 280
arvelexin (**6**)	12.3	186	209 $[M + Na]^+$ (14), 187 (100), 160 (33), 147 (65), 132 (5)	ND[c]	220, 266, 280, 290
rutalexin (**10**)	12.9	232	255 $[M + Na]^+$ (5), 233 (100), 192 (17), 148 (17)	231 (100), 174 (4)	213, 242, 275
dehydro-4-methoxycyclobrassinin (**18**)	14.2	262	263 (100)	ND[c]	210, 240, 270, 410
brassicanate A (**9**)	14.4	221	244 $[M + Na]^+$ (28), 222 (8), 190 (100)	220 (100), 205 (7)	220, 238, 268, 300
caulilexin A (**2**)	15.3	223	246 $[M + Na]^+$ 224 (31), 176 (100)	222 (5), 176 (100)	213, 252, 318
caulilexin C (**7**)	16.3	186	187 (49), 160 (100), 130 (20)	ND[c]	220, 272
1-methoxy-3-methoxymethylindole (**23**)	17.1	191	192 (5), 176 (6), 160 (100), 145 (95)	ND[c]	220, 272
brassinin (**11**)	18.3	236	259 $[M+ Na]^+$ (100), 237 (2), 176 (2), 130 (51)	236 (100), 190 (9), 172 (7)	220, 272
4-methoxybrassinin (**12**)	19.6	266	319 (100), 160 (14), 130 (3)	ND[c]	220, 270
1,1′-diindolylmethane (**27**)	22.8	246	247 (66), 245 (30), 130 (100)	ND[c]	220, 270
cyclobrassinin (**14**)	23.1	234	235 (37), 187 (15), 162 (100)	233 (8), 190 (37), 172 (9), 161 (100)	205, 229, 285, 294
4-methoxycyclobrassinin (**15**)	23.2	264	265 (100), 217 (10), 192 (80)	ND[c]	218, 268
1-methoxybrassinin (**13**)	23.6	266	289 $[M + Na]^+$ (25), 267 (49), 235 (36), 219 (10),160 (100), 146 (68), 128 (30), 117 (87)	265 (100), 220 (47), 190 (48), 144 (68)	218, 268
1-indolyl-1′-(1-methoxyindolyl)methane (**28**)	27.9	276	277 (11), 275 (100), 130 (20)	ND[c]	220, 270
sinalbin B (**16**)	33.1	266	265 (40), 233 (100), 217(8), 192 (60), 160 (26)	ND[c]	231, 275
1,1′-di-(1-methoxyindolyl)methane (**29**)	34.8	306	307 (3), 305 (57), 276 (28), 275 (100), 145 (5)	ND[c]	220, 280
			Polar Metabolites[b]		
tyrosine (**43**)	1.6	181	182 (25), 165 (100), 136 (12)	181 (100), 164 (45), 136 (10)	220, 275
cytidine (**44**)	2.1	243	487 (100), 244 (14)	129 (9), 113 (100)	210, 266
adenine (**40**)	2.1	135	136 (100)	134	210, 260
adenosine (**41**)	2.2	267	268 (100), 136 (40)	533 (100), 314 (4), 267 (2)	220, 260
uridine (**42**)	3.6	243	ND[c]	287 (100), 243 (10), 113 (9)	210, 260
glucobrassicin (**31**)	4.7	447	339 (20), 190 (100)	477 (100)	225, 285
coniferin (**35**)	4.5	342	164 (100)	387 (100), 342 (5)	216, 260, 295
tryptophan (**45**)	5.4	204	205 (5), 188 (100), 146 (25)	204 (100)	220, 280
4-hydroxyglucobrassicin (**30**)	5.6	464	465 (10), 265 (100)	463 (100)	220, 280
syringin (**36**)	5.6	372	767 (100), 194 (35), 162 (12), 134 (2)	417 (100)	220, 265
gluconasturtiin (**34**)	6.5	423	424 (30), 344 (50), 182 (100), 105 (80)	422 (100)	208, 236
4-methoxyglucobrassicin (**32**)	6.7	477	399 (100), 319 (50), 237 (80)	477 (100)	226, 275, 290
roseoside (**39**)	7.2	386	ND[c]	432 (100)	215, 260, 248
dihydroascorbigen (**37**)	8.9	307	308 (100), 262 (30), 130 (20)	613 (100), 307 (25)	220, 281, 290
neoglucobrassicin (**33**)	13.9	477	479 (7), 399 (100), 237 (80), 130 (70)	477 (100)	219, 265, 290
dihydroneoascorbigen (**38**)	13.9	337	338 (100), 307 (20), 174 (5), 130 (5)	673 (100), 338 (5)	222, 290

[a] HPLC solvent system: method NP-MS. [b] HPLC solvent system: method PP-MS. [c] ND = not detected.

in control roots in different concentrations. Lower polarity phytoanticipins, including indolyl-3-acetonitriles **5**−**7** and ascorbigens **19** and **20**, were present in higher concentrations in infected roots at earlier stages of infection (**Figure 1**), whereas phytoalexins **1**−**4** and **8**−**18** were produced at later stages of infection (**Figure 1**). Of particular note is the much higher concentration of cyclobrassinin (**14**), although at the present time, the significance of this result is not understood. By contrast, polar phytoanticipins such as the indolyl glucosinolates **31**, **32**, and **33** were present at higher concentrations in control roots five and six weeks after planting, whereas at earlier stages, infected and control roots had similar concentrations (**Figure 9**). Previously, neither the phytoalexin camalexin nor indole glucosinolates were shown to be crucial factors influencing gall development in roots of *A. thaliana* infected with *P. brassicae* (*8*).

Table 2. Antifungal Bioassay[a] of Metabolites **15**, **17**−**21**, **23**, **26**, **37**, and **38** against *Rhizoctonia solani*, *Alternaria brassicicola*, *Sclerotinia sclerotiorum* (% of Mycelial Growth Inhibition)

	R. solani			*A. brassicicola*			*S. sclerotiorum*		
compounds	0.50 mM	0.25 mM	0.10 mM	0.50 mM	0.25 mM	0.10 mM	0.50 mM	0.25 mM	0.10 mM
4-methoxycyclobrassinin (**15**)	56 ± 5	30 ± 2	20 ± 2	0	0	0	82 ± 2	51 ± 10	24 ± 2
dehydrocyclobrassinin (**17**)	39 ± 9	22 ± 5	14 ± 2	0	0	0	27 ± 1	14 ± 4	5 ± 4
4-methoxydehydrocyclobrassinin (**18**)	42 ± 9	27 ± 2	16 ± 3	0	0	0	27 ± 1	18 ± 4	11 ± 6
ascorbigen (**19**)	24 ± 6	19 ± 3	0	0	0	0	42 ± 12	36 ± 2	36 ± 6
neoascorbigen (**20**)	14 ± 3	11 ± 1	0	0	0	0	34 ± 5	22 ± 5	18 ± 2
3-methylsulfonylmethylindole (**21**)	0	0	0	0	0	0	24 + 2	18 ± 2	13 ± 4
1-methoxy-3-methoxymethylindole (**23**)	56 ± 10	38 ± 7	20 ± 9	77 ± 2	46 ± 6	24 ± 3	47 ± 4	34 ± 8	14 ± 2
1-methoxyindole-3-carboxaldehyde (**26**)	74 ± 6	43 ± 6	21 ± 7	74 ± 5	38 ± 6	21 ± 6	49 ± 2	27 ± 2	18 ± 6
dihydroascorbigen (**37**)	59 ± 5	32 ± 9	8 ± 5	0	0	0	24 ± 1	20 ± 7	9 ± 2
dihydroneoascorbigen (**38**)	18 ± 3	11 ± 5	10 ± 3	0	0	0	22 ± 4	17 ± 8	10 ± 2

[a] Percentage of mycelial growth inhibition calculated as reported in Materials and Methods (each value represents the mean % and standard deviation).

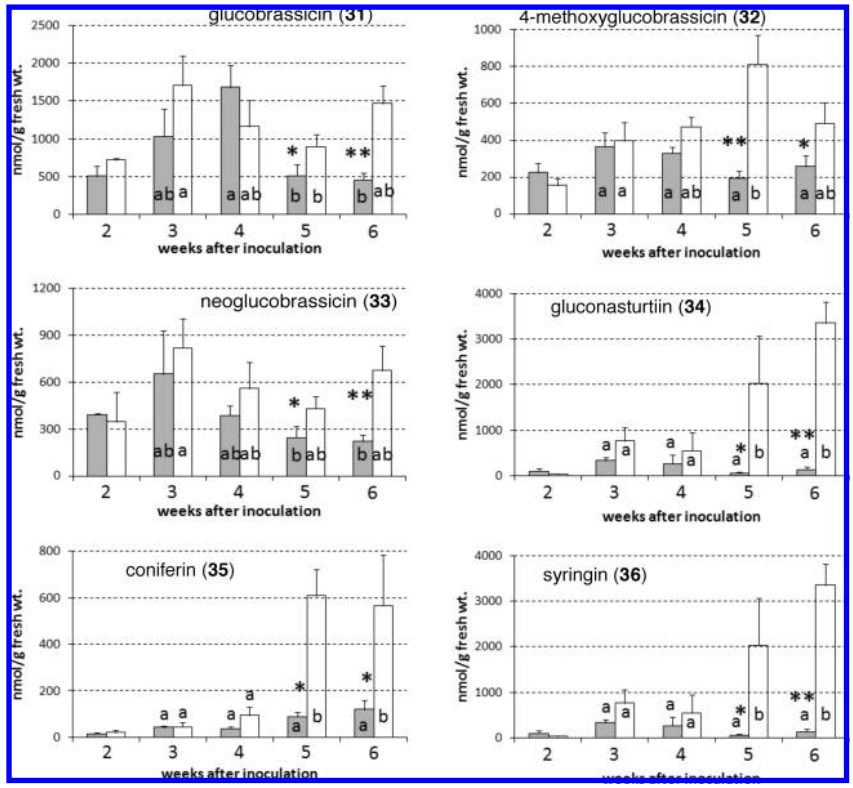

Figure 9. Accumulation of polar (PP) metabolites in roots of canola (*Brassica napus* cv. Westar) infected with *Plasmodiophora brassicae* over a six-week period. HPLC analysis is as described in Materials and Methods. Gray bars, infected roots; open bars, control roots. For statistical analysis, one-way ANOVA tests were performed (for control and infection each) followed by Tukey's test with adjusted α set at 0.05; $n = 3$; error bar, standard deviation (same letters indicate nonsignificant differences); Student's *t*-test, * $P < 0.05$; ** $P < 0.01$.

Although enzymatic hydrolysis of indolyl glucosinolates leads to a number of products that includes nitriles **5**, **6**, and **7** and ascorbigens **19** and **20**, since the concentrations of indolyl glucosinolates **31**, **32**, and **33** are substantially higher than those of the nitriles **5**−**7**, direct correlations between both groups are not expected nor observed. However, since tryptophan is the primary precursor of the brassica phytoalexins and indolyl phytoanticipins, a change in its concentration in infected and control roots would be expected, albeit not observed at any stage of root growth. The relatively low concentration of tryptophan might reflect its fast turnover during the infection. Also, indolyl-3-acetic acid (IAA) was not detected in quantifiable amounts because of its low concentration in any of the root extracts (<0.5 nmol/g of fresh tissue). These results are consistent with previous reports showing that IAA is produced in significantly larger amounts in infected roots of crucifers at earlier stages of infection, before any substantial metabolic changes occur (*3*).

Also, this work revealed gluconasturtiin (**34**) as the major aromatic glucosinolate produced in the roots of canola in control samples, after five and six weeks of growth, but its concentration in infected roots is significantly lower. Although intriguing, whether this difference is due to its degradation by the pathogen or plant or a down regulation of its biosynthetic pathway is yet to be determined. Similarly, the significance of substantially higher concentrations of the phenylpropanoids syringin (**35**) and coniferin (**36**) in older control canola roots relative to infected roots remains to be understood. Previously, syringin (**35**) and coniferin (**36**) were identified in *A. thaliana* roots infected with *Pythium sylvaticum* though their biological functions were not assigned (*18*). Both syringin (**35**) and coniferin (**36**) were produced in larger amounts in control roots of *A. thaliana* but in ca. 50% lower quantities than those determined in our work. Considering that a reduction in caffeoyl-CoA *O*-methyltransferase production in canola roots infected with *P. brassicae* was

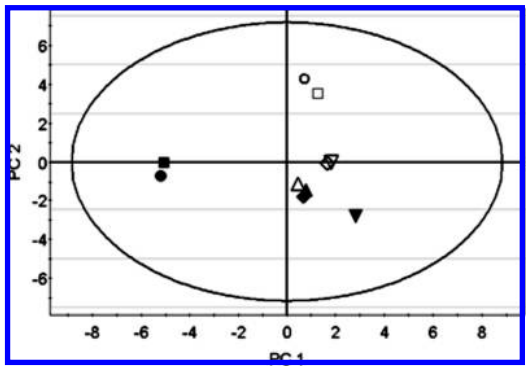

Figure 10. Principal component analysis (PCA, score plot) of extracts of canola (*Brassica napus* cv. Westar) roots infected with *Plasmodiophora brassicae* and control roots based on the absolute quantities of 17 secondary metabolites; filled wingdings, infected roots; open wingdings, control roots; ▲(Δ), 2 weeks; ▼(∇), 3 weeks; ♦(◊), 4 weeks; ●(○), 5 weeks; ■(□), 6 weeks.

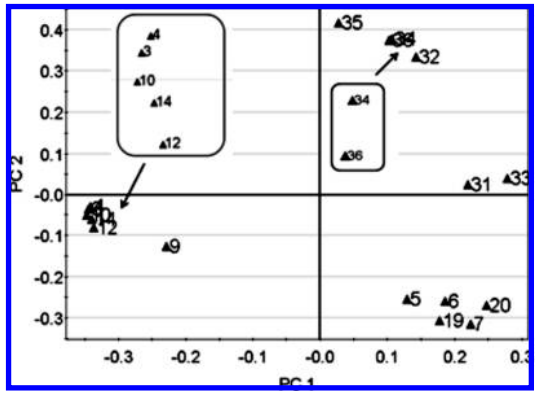

Figure 11. Principal component analysis (PCA, loading plot) of PC1 vs PC2 based on the absolute quantities of 17 secondary metabolites of extracts of canola (*Brassica napus* cv. Westar) roots infected with *Plasmodiophora brassicae*. Numbers represent the structure numbers shown in **Figures 5** and **6**.

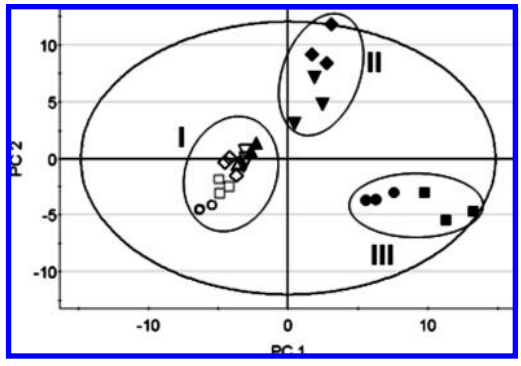

Figure 12. Principal component analysis (PCA, score plot) of canola (*Brassica napus* Westar) roots infected with *Plasmodiophora brassicae* and control roots based on the relative quantities of 107 secondary metabolites; filled wingdings, infected roots; open wingdings, control roots; ▲(Δ), 2 weeks; ▼(∇), 3 weeks; ♦(◊), 4 weeks; ●(○), 5 weeks; ■(□), 6 weeks.

previously observed (*7*) and that caffeic acid is a precursor of coniferin (**36**), our results are consistent with a reduction in root lignin biosynthesis due to infection. Interestingly, it was determined that coniferin (**36**) and syringin (**35**) accumulation in roots of *A. thaliana* was light induced and that this accumulation might be due to a redirection into the lignin and hydroxycinnamic acid biosynthetic pathways (*19*). The concentrations of syringin (**35**) and coniferin (**36**) detected in those light induced roots were about 2-fold higher than those observed in these experiments using canola roots.

Multivariate data analysis using PCA revealed distinct metabolic responses of canola to *P. brassicae* infection within a 6-week period (**Figures 10**−**12**). A clear discrimination between early and late harvest days shows a time dependent shift between the metabolic regulation of phytoanticipins and phytoalexins. Our previous work with the biotroph *A. candida* revealed that leaves of canola and rapeseed (*B. rapa* L.) also produced phytoalexins, phytoanticipins, and a number of polar metabolites (*10*). In that work, the interactions of plant cultivars with four races of *A. candida* suggested that this pathogen was able to elude the plant defense mechanisms by redirecting the phytoalexin biosynthetic pathway. However, considering the current data (due to a lack of *in vitro* cultivability of this pathogen, a direct effect of phytoalexins or other metabolites could not be established), it would be premature to suggest that *P. brassicae* might use a similar strategy to overcome plant defenses.

In conclusion, the interaction of canola and *P. brassicae* appears to provide a good model system to investigate the regulation of phytoanticipins and phytoalexins, and mechanisms used by the biotroph to overcome host defenses. The analytical methods developed allowed the simultaneous assessment of different metabolic pathways involving a large number of metabolites produced in infected roots. Distinct defense pathways involving up and down regulation of the biosynthesis of phytoanticipins and phytoalexins were revealed through PCA analysis. In addition, this study demonstrates for the first time that canola roots under biotrophic attack are able to produce a complex blend of phytoalexins and other antimicrobial metabolites as a defensive response. Considering the worldwide occurrence and significance of clubroot disease in the oilseeds canola and rapeseed, it would be of great interest to analyze the interactions of tolerant lines of canola/rapeseed with different pathotypes of *P. brassicae*.

ABBREVIATIONS USED

cv., cultivar; NP, nonpolar; NP-MS, NP-mass spectrometry; PP, polar; PP-MS, PP-mass spectrometry; PCA, principal component analysis.

ACKNOWLEDGMENT

We acknowledge the technical assistance of Ravi S. Gadagi and Ambuj Jha to grow and extract infected plant tissues.

Supporting Information Available: Principal component analysis data sets. This material is available free of charge via the Internet at http://pubs.acs.org.

LITERATURE CITED

(1) Bailey, J. A.; Mansfield, J. W. *Phytoalexins*; Blackie and Son: Glasgow, U.K., 1982; p 334.
(2) Pedras, M. S. C.; Zheng, Q. A.; Sarma-Mamillapalle, V. K. The phytoalexins from Brassicaceae: structure, biological activity, synthesis and biosynthesis. *Nat. Prod. Comm.* **2007**, *2*, 319–330.
(3) Cao, T.; Tewari, J.; Strelkov, S. E. Molecular detection of *Plasmodiophora brassicae*, causal agent of clubroot of crucifers, in plant and soil. *Plant Disease* **2007**, *91*, 80–87.
(4) Ludwig-Müller, J.; Schuller, A. What can we learn from clubroots: alterations in host roots and hormone homeostasis caused by *Plasmodiophora brassicae*. *Eur. J. Plant Pathol.* **2008**, *12*, 291–302.

(5) Ando, S.; Asano, T.; Tsushima, S.; Kamachi, S.; Hagio, T.; Tabei, Y. Changes in gene expression of putative isopentenyltransferase during clubroot development in Chinese cabbage (*Brassica rapa* L.). *Physiol. Mol. Plant Pathol* **2005**, *67*, 59–67.

(6) Ishikawa, T.; Okazaki, K.; Kuroda, H.; Itoh, K.; Mitsui, T.; Hori, H. Molecular cloning of *Brassica rapa* nitrilases and their expression during clubroot development. *Mol. Plant Pathol.* **2007**, *8*, 623–637.

(7) Cao, T.; Srivastava, S.; Rahman, M. H.; Kav, N. N. V.; Hotte, N.; Deyholos, M. K.; Strelkov, S. E. Proteome-level changes in the roots of *Brassica napus* as a result of *Plasmodiophora brassicae* infection. *Plant Sci.* **2008**, *174*, 97–115.

(8) Siemens, J.; Glawischnig, E.; Ludwig-Müller, J. Indole glucosinolates and camalexin do not influence the development of the clubroot disease in *Arabidopsis thaliana*. *J. Phytopathol.* **2008**, *156*, 332–337.

(9) Mendgen, K.; Hahn, M. Plant infection and the establishment of fungal biotrophy. *Trends Plant Sci.* **2002**, *7*, 352–356.

(10) Pedras, M. S. C.; Zheng, Q. A.; Gadagi, R. S.; Rimmer, S. R. Phytoalexins and polar metabolites from the oilseeds canola and rapeseed: differential metabolic responses to the biotroph *Albugo candida* and to abiotic stress. *Phytochemistry* **2008**, *69*, 894–910.

(11) Strelkov, S. E.; Tewari, J. P.; Smith-Degenhardt, E. Characterization of *Plasmodiophora brassicae* populations from Alberta, Canada. *Can. J. Plant Pathol.* **2006**, *28*, 467–474.

(12) Pedras, M. S. C.; Adio, A. M.; Suchy, M.; Okinyo, D. P.; Zheng, Q. A.; Jha, M.; Sarwar, M. G. Detection, characterization and identification of crucifer phytoalexins using high-performance liquid chromatography with diode array detection and electrospray ionization mass spectrometry. *J. Chromatogr., A* **2006**, *1133*, 172–183.

(13) Monde, K.; Tamura, K.; Takasugi, M.; Kobayashi, K.; Somei, M. Dehydro-4-methoxycyclobrassinin, a sulfur-containing phytoalexin isolated from Turnip *Brassica campestris* L. ssp. *rapa*. *Heterocycles* **1994**, *38*, 263–267.

(14) Licari, J. J.; Dougherty, G. Reactions of gramine with sulfur compounds. *J. Am. Chem. Soc.* **1954**, *76*, 4039–4040.

(15) McCarthy, J. R.; Matthews, D. P.; Paolini, J. P. Reaction of sulfoxides with diethylaminosulfur trifluoride: fluoromethyl phenyl sulfone, a reagent for the synthesis of fluoroalkenes. *Org. Synth.* **1998**, *9*, 446–449.

(16) Latxague, L.; Gardrat, C.; Coustille, J. L.; Viaud, M. C.; Rollin, P. Identification of enzymatic degradation products from synthesized glucobrassicin by gas chromatography mass spectrometry. *J. Chromatogr.* **1991**, *586*, 166–170.

(17) Yudina, L. N.; Korolev, A. M.; Reznikova, M. I.; Preobrazhenskaya, M. N. Investigation of neoascorbigen. *Chem. Heterocycl. Compd.* **2000**, *36*, 141–151.

(18) Bednarek, P.; Schneider, B.; Svatos, A.; Oldham, N. J.; Hahlbrock, K. Structural complexity, differential response to infection, and tissue specificity of indolic and phenylpropanoid secondary metabolism in *Arabidopsis* roots. *Plant Physiol.* **2005**, *138*, 1508–1570.

(19) Hemm, M. R.; Rider, S. D.; Ogas, J.; Murry, D. J.; Chapple, C. Light induces phenylpropanoid metabolism in *Arabidopsis* roots. *Plant J.* **2004**, *38*, 765–778.

Received for review July 17, 2008. Revised manuscript received September 1, 2008. Accepted September 2, 2008. Support for this work was obtained from the Natural Sciences and Engineering Research Council of Canada (Accelerator Grants for Exceptional New Opportunities to M.S.C.P.), Canada Foundation for Innovation, Canada Research Chairs Program (M.S.C.P.), and the University of Saskatchewan.

JF802192F